

Fatigue Properties under Constant Stress/Variable Stress Amplitude and Coaxing Effect of Acicular Ductile Iron and 42 CrMo4 Steel

A.R. I. Kheder^a, N. M. Jubeh^{*b}, E. M. Tahah

^aAl-Balqa' Applied University, Faculty of Engineering, Department of Materials and Metallurgical Engineering, Al-Salt, Jordan

^bAl-Balqa' Applied University, Faculty of Engineering Technology, Department of Mechanical Engineering, Amman, Jordan

Abstract

Fatigue characteristics of as-cast acicular ductile iron (ASGI) produced by alloying and controlled cooling and as-rolled 42CrMo4 steel were studied. Rotating bending fatigue tests at a stress ratio of $R = -1$ was employed. Tests included constant stress amplitude loading, variable stress amplitude high-low, low-high loading and coaxing. $S - N$ curves were established and fatigue strengths were determined, (450 N/mm² for ASGI, 460 N/mm² for steel). The variable stress amplitude loading, high-low, showed high N_T/N_f for the materials, while variable stress amplitude loading, low-high showed a decrease in N_T/N_f for steel and only small improvement for ASGI (N_T = total stress cycles in variable stress amplitude, N_f = stress cycles in constant stress amplitude to failure). Both materials showed coaxing effect, pronounced more in ASGI. The crack propagation rate determined using Paris equation at constant stress amplitude for ASGI was $da/dN = 2.0 * 10^{-5} (\Delta K)^{2.6902}$ and for steel it was $da/dN = 1.0 * 10^{-6} (\Delta K)^{3.5205}$.

© 2011 Jordan Journal of Mechanical and Industrial Engineering. All rights reserved

Keywords: fatigue strength; as-cast ASGI; 42CrMo4 steel; constant stress; amplitude; variable stress amplitude; coaxing effect

1. Introduction

Spheroidal graphite cast irons (SGI) are generally used in as-cast condition or after relatively simple annealing or normalizing heat treatment [1]. Remarkable engineering properties and the full potential of the material can be achieved when the SGI is heat treated and converted to austempered ductile iron [2], but the cost of adding elaborate heat treatment facilities is high. An alternative method is to employ a controlled cooling schedule closely approximating the thermal schedule for austempering with suitable alloying elements [3-4]. The heat treatment conditions can be selected, either to produce a structure of upper bainite which combines high strength, ductility and toughness or lower bainite which is characterized by good wear resistance and high strength.

The austempered ductile iron has excellent toughness and wear-resistance and has been shown to have superior fatigue properties as well. The fatigue strength tests of gears showed that the bainitic ductile iron grades were superior to the pearlitic and quenched and tempered grade [5].

The fatigue strength of the materials is related to their tensile strength. The endurance ratio (ratio of unnotched fatigue strength to tensile strength) is approximately 0.45 for nodular graphite irons and compacted graphite irons [6]. Both nodular and compacted graphite irons do not exhibit the lack of notch sensitivity shown by the flake graphite cast irons because they do not contain the sharp-edge graphite flakes which act as internal notches in flake

graphite irons. Both types of irons are notch sensitive in fatigue. With a relatively sharp notch the fatigue limit is reduced to about a quarter of the tensile strength [7], various kinds of cast irons containing different graphite shapes were investigated and the influence of graphite shape on fatigue strength of cast iron was determined from stand points of the external effect, the notch effect of graphite and the effect of reduction of effective sectional area caused by graphite [8].

The matrix of cast iron is comparable to that of steel and thus can be in ferrite, pearlite and other phases possible in steel. The morphology of graphite in cast iron determines the type of cast iron and it is the controlling factor of the mechanical and physical properties of the cast iron.

This paper describes the fatigue strength and crack growth behavior of as-cast acicular spheroidal graphite cast iron. The results are compared with those of as-rolled steel, and discussed from several viewpoints and compared with the data available in the literature.

2. Experimental Procedure

In this study, specimens of acicular spheroidal graphite cast iron (ASGI) and 42CrMo4 steels were subjected to rotating bending fatigue tests. The ASGI specimens for fatigue tests and other mechanical properties were prepared from ingots produced by controlled cooling and alloying method [4]. They were tested in as-cast

* Corresponding author. e-mail: jubeh@wanadoo.jo

condition. The steel specimens for tests were prepared from steel rods of 40 mm diameter.

The preparation of the fatigue test specimens from ingots is shown in Fig. 1, CNC wire cutting machine was used for this purpose and then the square specimens were further machined to obtain the fatigue test specimens as shown in Fig. 2. The fatigue specimens from rolled steel were machined directly to the required dimensions, Fig. 2. The final machining of the fatigue specimens were carried out on CNC lathe machine. To obtain smooth surface, the fatigue test specimens were ground using emery papers 320, 500, 800, and 1000 grades and then diamond paste of $\frac{2}{3}$ μm particle size was utilized for polishing the surface. The average surface roughness of $R_{\text{max}} = 1.89 \mu\text{m}$ was obtained and taken into consideration. The chemical composition and mechanical properties of the materials employed are given in Tables 1 and 2 respectively.

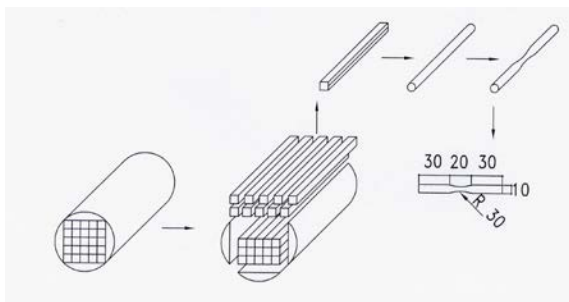


Figure 1: Preparation of the fatigue specimen of the ASGI.

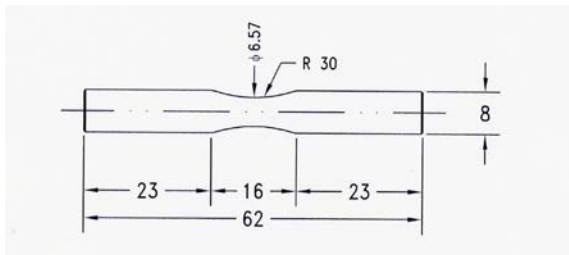


Figure 2: Fatigue specimen.

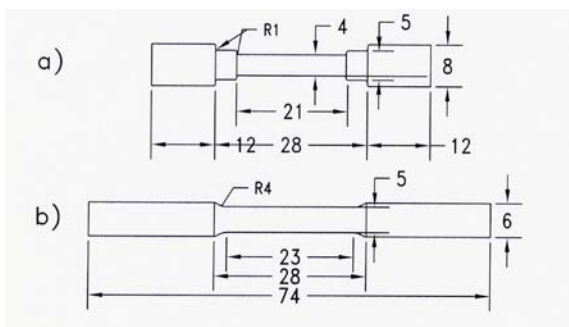


Figure 3: Tensile test specimen:
 a) ASGI according to ISO 1083.
 b) Steel according to DIN 50125.

Table 1: Chemical composition of the materials.

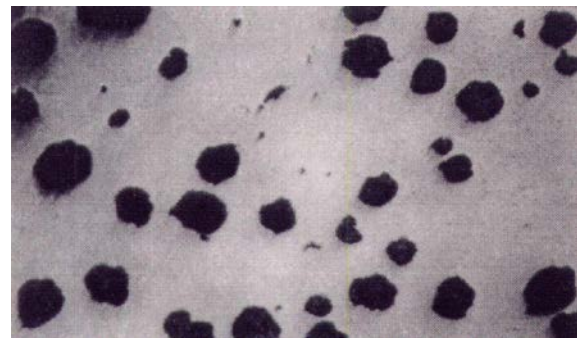
Elements	C	Si	Mn	Cr	Ni	Mo	S	P	Mg
ASGI	3.3	2.8	0.2	0	2.8	0.2	0.01	0	0.033
Steel 42CrMo4	0.4	0.2	0.5	0.9	0.2	0.1	0.03	0	-

Table 2: Mechanical properties of the materials

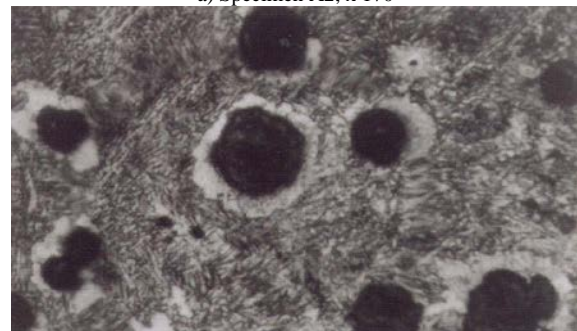
Mechanical properties	Yield strength N/mm ²	Tensile strength N/mm ²	Hardness HBN	Elongation %
ASGI	780	1050	370	5.5
Steel 42CrMo4	885	1096	217	10

To determine the tensile properties of the materials, specimens were machined to the dimensions given in Fig. 3 according to ISO 1083 for ASGI and DIN 50125 for steel.

The ASGI specimens were subjected to microstructural examinations to determine the number of graphite nodules/mm² and the matrix microstructure. The matrix microstructure consisted of about 95% bainite and about 5% retained austenite. These percentages were estimated by applying the direct comparison method [9]. The constituents of the microstructure are shown in Fig. 4 for ASGI in unetched and etched conditions. The details of the graphite nodules across the cross section of the ingot, such as the number of nodules/mm², the nodule size and the area fraction of the nodules, as well as the hardness variation of the structure with distance, are shown in Figs. 5 and 6. The structure of the steel was mainly pearlite.



a) Specimen A2, x 170



b) Specimen A4, x 270

Figure 4: a) Graphite nodules in as-cast ASGI, unetched, x 170.
 b) Graphite nodules and the matrix structure in as-cast ASGI, etched, x 270.

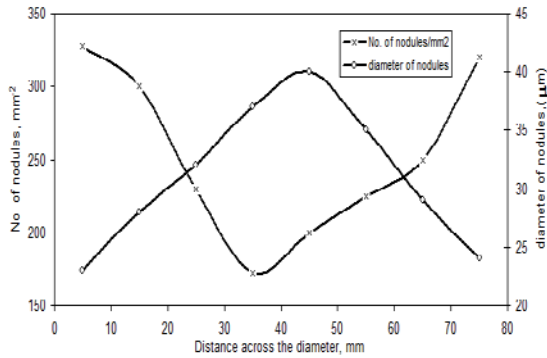


Figure 5: Change of the number of graphite nodules/mm² and their diameter with the distance.

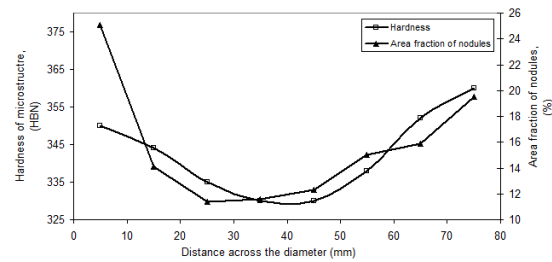


Figure 6: Change on the area fraction of graphite and hardness with the distance.

Fatigue tests were carried out using the rotating bending fatigue machine with a stress ratio of R= -1. The tests were divided into three groups:

- Constant stress amplitude fatigue tests on specimens of as-cast ASGI, as-rolled steel.
- Variable stress amplitude fatigue tests including two-step, low-high and high-low loading tests on specimens of as-cast ASGI and as-rolled steel.
- Coaxing effect on specimens of as-cast ASGI and as-rolled steel.

The fatigue crack propagation was followed up by using plastic replica technique. Cellulose acetate foils of 35µm thickness were employed for this purpose. The foils were cut into strips suitable for sticking on the surface of the specimens after wetting by acetone and left for 3-4 minutes for drying, then the replicas were lifted from the surface carefully and fixed between two glass slides for observations and crack length measurements using optical microscope.

To study the coaxing effect, some of the fatigue specimens were tested at stresses 3 MPa below the fatigue limits of the concerned material for duration of 7x10⁶ cycles, then loading the specimens to stresses more than the fatigue limits and measuring the number of cycles to failure. The results obtained in this way were compared with the number of cycles to failure under constant stress amplitude at the stresses above the fatigue limits as shown in Table 3.

Table 3: Data of the coaxing effect.

	σ_1 (MPa)	σ_2 (MPa)	N_1 under σ_1	N_2 under σ_2	N_f under σ_2 Constant stress	N_2/N_f
ASGI	447	520	7 000 000	1 050 000	93 000	11.29
42 CrMo4	457	520	7 000 000	880 000	200 000	4.4

3. Results and Analysis

3.1. Results of constant amplitude loading:

From the test results under constant stress amplitude loading tests, the stress-stress cycle (S-N) curves were drawn for the specimens of as-cast ASGI and as-rolled 42CrMo4 steel. These results are shown in Fig. 7. These curves can be expressed mathematically as follows:

For as-cast ASGI:

$$\Delta\sigma = 957.56 N_f^{-0.049} \tag{1}$$

For as-rolled 42CrMo4 steel

$$\Delta\sigma = 1387.9 N_f^{-0.073} \tag{2}$$

Where

$$\Delta\sigma = \sigma_{\max} - \sigma_{\min}$$

The fatigue limits (σ_w) for the materials used were obtained from the results given in Table 4 and Fig. 7, and they are: 450 N/mm² for as-cast ASGI and 460N/mm² for as-rolled steel. There are more up-to-date and elaborate models of expressing the fatigue data in the literature [10, 11, &12]. These models can lead to a better fit and provide more appropriate information when compared with the traditional model applied in this study. Increasing the number of specimens will lead to a better fit and more accurate results. The σ_w for as-cast ASGI and for as-rolled steel are quite reasonable when compared with $\sigma_w = 380$ MPa of S 45C quenched and tempered steel used by [13] reflecting the strength of both materials, particularly the ASGI specimens of bainitic structure.

Table 4: Data of stress ($\bar{\sigma}$) – number of stress cycles (N), for ASGI and 42 CrMo4 steel.

Specimen Number	ASGI		42 CrMo4 steel	
	$\bar{\sigma}$ (N/mm ²)	N	$\bar{\sigma}$ (N/mm ²)	N
1	625	44000	700	44200
2	600	46000	650	61000
3	550	73000	625	110000
4	520	93000	600	150000
5	500	160000	550	185000
6	500	220000	520	200000
7	485	2760000	500	400000
8	475	2800000	500	370000
9	460	6800000	470	7200000
10	450	10000000 No failiure	460	10000000 No failiure
11	400	10000000 No failiure	450	10000000 No failiure

The endurance ratios (σ_w/σ_{uts}) of the materials concerned are: 0.428 and 0.419 for as-cast ASGI and as-rolled steel respectively, where σ_{uts} = ultimate tensile stress. The values for endurance ratio of ASGI and rolled steel are in quite reasonable agreement with published data in [6,8, &14]. The ratios for ASGI and rolled steel are very close indicating that the graphite nodules effect as internal notches in ASGI is negligible emphasizing the conclusion drawn by the authors in [8], where they state that the influence of the notch effect of graphite is far smaller than what has been considered before. This influence can be recognized slightly in case of flake graphite cast iron, but hardly in case of spheroidal graphite cast iron. Many short cracks were formed and were stopped from propagation, at graphite nodules in ASGI after duration of 7×10^6 cycles at stress levels just below σ_w .

The data given in Figs. 5 and 6 are of important value in castings of parts with different thicknesses or diameters which graphite nodule number, size, and volume fraction, as well as the hardness of the structure vary, hence other mechanical properties will vary and should be considered. The data available in this area is very rare, and the results obtained in this study were encouraging.

3.2. Results of variable amplitude loading:

Specimens of as-cast ASGI and as-rolled 42CrMo4 steel were subjected to variable stress amplitude fatigue tests, namely two-steps, low-high (L-H) and high-low (H-L) at initial loading of about $N_1/N_f = 0.25$ where N_1 = number of the stress cycles at initial loading, and N_f = number of the stress cycles at failure. The results are included in Table 4. It is clear from the results that the variable amplitude loading mode H-L leads to higher fatigue life in both materials, while L-H amplitude loading mode results in lower fatigue life in case of as-rolled steel, and in as-cast ASGI there was an increase but not as high as in loading mode H-L, the increase was relatively small compared with the results of constant loading mode at the same stress level.

The increase in fatigue life in case of H-L loading can be explained in terms of formation of large plastic zone at the tip of the crack which delays the crack growth rate at the lower stress level and increases the fatigue life. A reason for the increase of the fatigue life of ASGI specimens in loading mode L-H rather than in steel is the high closure rate of the crack under the higher stress of 600 MPa after changing from 500 MPa which is larger than the closure rate of the crack in tests at constant stress amplitude test. This can be also due to the higher values of the stress intensity factor K than the threshold level which leads to a decrease in the force (stress) responsible of the crack growth at 600 MPa and results in a ratio of $NT/N_f > 1$. Therefore the value of the NT/N_f for ASGI is larger than the value for 42CrMo4 steel in variable loading mode L- H, (NT is the sum of stress cycles at both stress levels, $NT = N_1 + N_2$, and N_f is the number of stress cycles to failure at constant stress amplitude).

3.3. Results of coaxing effect:

Coaxing effect was studied on specimens of as-cast ASGI and as-rolled 42CrMo4 steel under the loading mode, two steps, L-H. The results for ASGI are shown in Fig. 8. First the fatigue tests were carried out at stresses 3 MPa below σ_w of both materials for a period enough to

create short cracks to appear which are not able to propagate, and then the specimens were subjected to stresses higher than σ_w of both materials. The coaxing effect means an increase of the fatigue strength or fatigue life after testing the specimens at stresses below σ_w and then above σ_w of the concerned material.

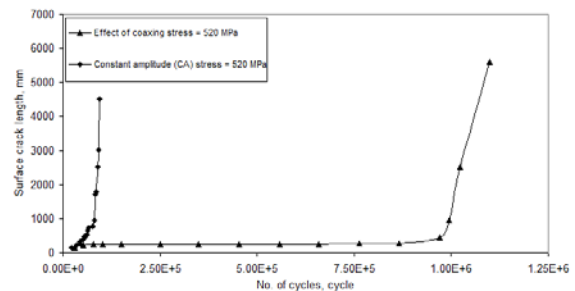


Figure 8: Coaxing effect in as-cast ASGI.

Both materials showed this phenomenon after subjecting the fatigue specimens to initial stress of 447 MPa and 457 MPa for as-cast ASGI and as-rolled 42CrMo4 steel respectively for a period of 7×10^6 cycle. From the results given in Fig. 8 and Table 4, the as-cast ASGI specimens failed after 9.3×10^4 cycles at constant stress amplitude of 520 MPa, while in L-H loading cycle 447-520 MPa the number of cycles to failure was 1.05×10^6 which gives a ratio of $N_2/N_f = 1.05 \times 10^6 / 9.3 \times 10^4 = 11.29$. Similar calculation for as-rolled steel cycled within the stress range of 457-520 MPa and tested at constant stress amplitude of 520 MPa gives a value of $N_2/N_f = 8.8 \times 10^5 / 2 \times 10^5 = 4.4$. In a recent study of the coaxing effect in spheroidal graphite cast iron (SGI) and compacted graphite cast iron (CGI), the following values were obtained: $N_2/N_f = 8.96$ for SGI and 7.34 for CGI, which are of the similar order reported in this work indicating a phenomenon of the same cause [15]. This effect is clearly shown in Fig. 8 for ASGI. The more positive response of the as-cast ASGI to coaxing effect may be related to the higher closure rate of the cracks and the graphite particles acting as obstacles against the crack propagation as shown in Fig. 9, besides the strain aging effect in ferrous materials [13, 16]. The SEM micrographs show clearly the path of the crack propagation which is between the graphite nodules after it has started at the surface of the fatigue specimen. Some branching can be seen, but the main crack is obvious.

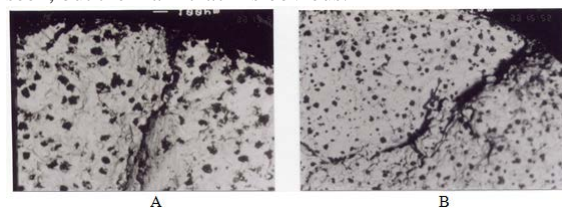


Figure 9: SEM micrographs showing the Crack propagation between the graphite nodules in the acicular ASGI.

A. 600 MPa, $\times 80$

B. 520 MPa, $\times 33$

The crack propagation rate for both materials was calculated according to Paris equation [17], for constant stress amplitude:

$$da/dN = C * (\Delta K)^n \quad (3)$$

Where C and n are constants, ΔK is the average stress intensity factor.

The constants were estimated by applying the least square method and the equations obtained are:

For as-cast ASGI

$$da/dN = 2.0 * 10^{-5} * (\Delta K)^{2.6902} \quad (4)$$

For as-rolled steel

$$da/dN = 1.0 * 10^{-6} * (\Delta K)^{3.5205} \quad (5)$$

The values for constant C for both materials are relatively larger when compared with the C values reported for spheroidal graphite iron, but the values for the constant n are close (n=3.3 to 5) [18, 19].

This study shows the different behavior of the crack propagation in as-cast ASGI and as-rolled steel specimens, because the crack propagation paths are different. In ASGI the crack propagates mainly between the graphite nodules, as shown in Fig. 9. Apparently the graphite nodules provide obstacles against the crack propagation besides other obstacles such as the various phases present in the microstructure, like bainite, martensite, retained austenite and the grain boundaries. In steel the microstructural barriers are the different phases, phase and grain boundaries, carbide particles and dislocations. The presence of graphite nodules increases the threshold stress determined by crack tip blunting during the crack transfer from the matrix to the graphite particles while crack transfer from graphite into matrix occurs if the $\Delta K \geq \Delta K_{th}$ for the matrix [20].

It was noted that there are major cracks and secondary cracks. At initial stages of the fatigue tests it is difficult to distinguish between them but as the test proceeds a chief crack forms and its rate of propagation can be followed and measured while those minor cracks remain inactive until the specimen fails.

4. Conclusion

- Acicular spheroidal graphite cast iron produced by alloying and controlled cooling constitute an important type of ductile iron and has fatigue properties in as-cast condition similar to that of as-rolled 42CrMo4 steel. Their endurance ratios are, 0.428 and 0.419 respectively.
- The number of graphite nodules/mm², the area fraction of the graphite nodules (%) and the hardness of the microstructure decrease with the distance from the outer surface towards the center of the ingot, while the graphite nodule size increases in the same direction.
- The variable stress amplitude high-low mode leads to higher fatigue life for as-cast ASGI and as-rolled steel, while low-high amplitude loading mode results in lower fatigue life in case of steel and an increase in that of ASGI but not as high as in high- low loading mode.
- The as-cast ASGI and as-rolled 42CrMo4 steel showed coaxing effect; it was more pronounced in the former material.

5. Acknowledgment

The second author "N. M. Jubeh" would like to acknowledge the support of Al-Balqa Applied University during his sabbatical leave, which he spends at the Hashemite University; this research was carried out during this period.

References

- [1] I.C. Hugues, A.G. Fuller, R.A. Harding, "Austempered ductile irons – their significance and present applications". Foundry Trade Journal, 10, 1985, 277-286.
- [2] H.L. Morgan, "Introduction to foundry production and control of austempered ductile irons". British Foundryman, 80, part 2, 1987, 98-108.
- [3] J.F. Janowak, R.B. Grunlach, "Approaching austempered ductile iron properties by controlled cooling in the foundry". Int. Conf. on austempered ductile iron, Chicago, Illinois, USA, ASM, 63-69, 2-4 April 1984.
- [4] A.R.I. Kheder, G. Al-Marahleh, "Effect of controlled cooling on the mechanical properties and microstructure of alloyed acicular ductile cast iron". Sci. Bull. Fac. Eng., Ain Shams Univ., Vol. 39, No. 2, 2004, 529-540.
- [5] M. Johansson, "Austenitic-Bainitic Ductile Irons". AFS transaction, 85, 1977, 117-122.
- [6] G.F. Sergeant, E.R. Evans, "The production and properties of compacted graphite irons". British Foundryman, 71, May 1978, 115-124.
- [7] J. Powell, "A review of some recent work on compacted graphite irons". British Foundryman, 77, part 9, Nov 1984, 472-483.
- [8] T. Shiota, S. Komatsu, "Influence of notch and effective sectional area on fatigue strength of cast irons with various graphite shapes". Jap. J. of Materials, 27(294), 1978, 291-297.
- [9] Cullity B.D, Stock S.R. Elements of X-ray diffraction. 3rd Ed. Prentice Hall; 2001.
- [10] E. Castillo, A.S. Hadi, (1995), "Modeling lifetime data with application to fatigue models". Journal of the American Statistical Association, 90, 1995, 1041-1054
- [11] F.G. Pascual, W.Q. Meeker, "Estimating fatigue curves with the random fatigue limit model". Technometrics, 41, 1999, 277-302.
- [12] E. Castillo, A. Fernandez-Canteli, "A general regression model for lifetime evaluation and prediction". International Journal of Fracture, 107, 2001, 117-137.
- [13] S. Ishihara, A.J. McEvily, "A coaxing effect in the small fatigue crack growth regime". Scripta Materialia, Vol. 40, No. 5, 1999, 617-622.
- [14] Haruyoshi Sumimoto, Kokichi Nakamura, Yoshinori Umeda, "The relation between graphite structure and fatigue limit ratio, fatigue limit in CV, spheroidal graphite cast iron". Jap. J. of Foundry Soc. 105 Conf., Kobe City, May, 19, 1984, 279-285.
- [15] A.R.I. Kheder, G. Marahleh, "Effect of coaxing on the fatigue strength of SGI and CGP", to be published in J. Applied Science.
- [16] Silverleaf D.J. Fatigue design of machine components. 6th ed. Pergamon press;1971.
- [17] J.B. Chang, E. Kleven, "A review and assessment of fatigue crack growth rate relationships for metallic air frame

- materials". Fracture and failure analysis mechanics and applications, ASM, 1981, 35-53.
- [18] Shen-Chill Lee and Yin-Bean Chang., "Fracture toughness and crack growth rate of ferritic and pearlitic compacted graphite cast iron at 25°C and 150°C". Metallurgical transaction A, 22A, Nov-1991, 2645-2653.
- [19] A.R.I. Kheder, G. Marahleh, S. Al-Goussous, "Fatigue crack propagation in SGI and CGI". J. Applied Science, Vol. 5, No. 5, 2005, 862-867.
- [20] O.N. Romaniv, A.N. Tkach, "Experimental study and modeling of near threshold crack growth in nodular cast iron". Fatigue, 90, 1990, 2155-2160.